Fluorescence Behaviour of Dyes in Different Microenvironments

M.Sc. Thesis

By

Dulee Chand Saini

DEPARTMENT OF CHEMISTRY

INDIAN INSTITUTE OF TECHNOLOGY INDORE

May, 2022

Fluorescence Behaviour of Dyes in Different Microenvironments

A THESIS

Submitted in partial fulfilment of the
Requirements for the award of the degree

Of
Master of Science

By
Dulee Chand Saini

DEPARTMENT OF CHEMISTRY
INDIAN INSTITUTE OF TECHNOLOGY INDORE
May, 2022

Indian Institute of Technology, Indore

CANDIDATE'S DECLARATION

I hereby certify that the work which is being presented in the thesis entitled **Fluorescence Behaviour of Dyes in Different Microenviornments** in the partial fulfilment of the requirements for the award of the degree of **MASTER OF SCIENCE** and submitted in the **DEPARTMENT OF CHEMISTRY, Indian Institute of Technology Indore**, is an authentic record of my own work carried out during the time period from July, 2021 to May, 2022, under the supervision of Dr. Tushar Kanti Mukherjee, Associate Professor of IIT Indore.

The matter presented in this thesis has not been submitted by me for the award of any other degree of this or any other institute.

Dulee 26-05-22

Signature of the student with date
Dulee Chand Saini

This is to certify that the above statement made by the candidate is correct to the best of my/our knowledge.

Tushar kanti Mukherjee.

Signature of Thesis Supervisor

Date: 27/05/2022

Dulee Chand Saini has successfully given his M.Sc. Oral Examination held on **24-05-2022**

Tushar kanti Mukherjee.
Signature(s) of Supervisor(s) of MSc thesis
Date: 27/05/2022

Tushar kanti Mukherjee.
Convener, DPGC
Date: 27/05/2022

B.S.S 27/5/22
Signature of PSPC #1
Date:

Achaksaborty 27/5/2022
Signature of PSPC Member #2
Date:

ACKNOWLEDGEMENTS

With great pleasure I would like to express my deep sense of gratitude to my supervisor Dr. Tushar Kanti Mukherjee for giving me this opportunity to pursue research and believing in me. His constant guidance and support to complete this M.Sc. project. Further I would like to thank my PSPC members Dr. Satya S. Bulusu and Dr. Anjan Chakraborty for their support.

I would like to express my gratitude to **Prof. Suhash S. Joshi**, Director IIT Indore, for his continuous encouragement and support in every aspect.

I extend my heartiest thanks to my PhD mentor Mr. Shivendra Singh, for his constant selfless guidance and also Miss Bhawna for her valuable support.

I would like to thank the technical staff from SIC, IIT Indore, Mr. Kinny Pandey, Mr. Ghanashyam Bhavsar, Dr. Ravinder and Mr. Manish Kushwaha for their patience and timely technical support without which it was impossible to continue with my project work.

I would like to thank IIT Indore for infrastructure and all other help and lastly, I would express my deepest appreciation for my beloved my parents, throughout these years that I have studied.

DULEE CHAND SAINI
CHEMISTRY

Table of Contents

List of Figures

List of Schemes

List of Tables

ACRONYM

CdTe	Cadmium Tellurium
CD	Carbon Dot
DCM	Di Chloro Methane
DMSO	Di Methyl Sulphoxide
λ_{ex}	Excited wavelength
FTIR	Fourier Transform Infrared
IPA	Isopropyl Alcohol
LLPS	Liquid-Liquid Phase Separation
MSA	Mercaptosuccinic acid
ND	Nanodroplet
PDADMAC	Poly(diallyldimethylammonium chloride
PL	Photoluminescence
QD	Quantum Dot

NOMENCLATURE

°C	Degree centigrade
h	Hour
nm	Nanometer
µM	Micromolar
mM	Milimolar
mg	Milligrams
mL	Milliliter
M	Molar
rpm	Revolution per minute

Chapter 1

Introduction

1.1. Nanoscience and Nanotechnology

The study and application of extremely small objects, which are undetectable to the naked eye, and utilization of these nanomaterials in other branches of science, are known as nanoscience and nanotechnology. These nanomaterials exhibit unique physical and chemical properties due to their ultra-small size and large surface area. Considering these unique features, NPs can be used in a variety of applications like sensing, catalysis, bioimaging, light-emitting diodes (LEDs), drug delivery etc. NPs have attracted a lot of attention recently, and they're becoming an essential material in the development of new nanodevices that can be employed in a variety of physical, biological, medicinal, and pharmacological applications.

Nanoscience has already seen significant advancements and discoveries. Many questions have been answered and important discoveries have been made. Synthetic procedures for precisely modifying the shape, size, and characteristics of colloidal nanoparticles (NPs) have been well explored, and continuous advancements and improvements have been made to date. Many NPs superstructures have been constructed with new attributes and applications, emulating the behaviour of well-organised natural machines (e.g. proteins, enzymes, biopolymers). This concept has influenced various major domains, including energy and biology.

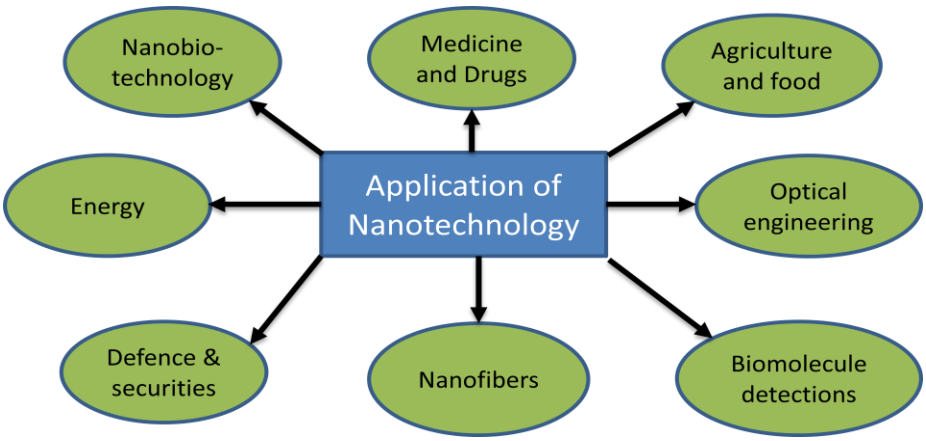

Figure 1.1 - Application of nanotechnology in various field

1.2. Nanoparticle

Nanoparticles (NPs) are very small materials that come under the size range of 1 to 100 nm. These are undetectable to the naked eye and reveal notably different physical and chemical properties compared to their bulk counterparts. The majority of NPs are made up of hundreds to thousands of atoms.

There has recently been a surge in interest in developing new multifunctional NPs with a variety of structures and activities. Precise control and tuning of nanoparticle size and morphology are one of the most essential criteria in nanoparticle design, which is important in a variety of domains including catalysis, biosensing[1], drug delivery[2,], nanoreactors, sensing, and biomedical research. As a result, there is a growing interest in the creation of organic, inorganic, and hybrid NPs with varying compositions, shapes, and particle sizes, resulting in the emergence of the nanotechnology research area.

1.3. Classification of NPs

Depending on their morphology, size and chemical characteristics, NPs are classified into several groups. Depending on chemical and physical features, some of the most well-known categories of NPs are listed below.

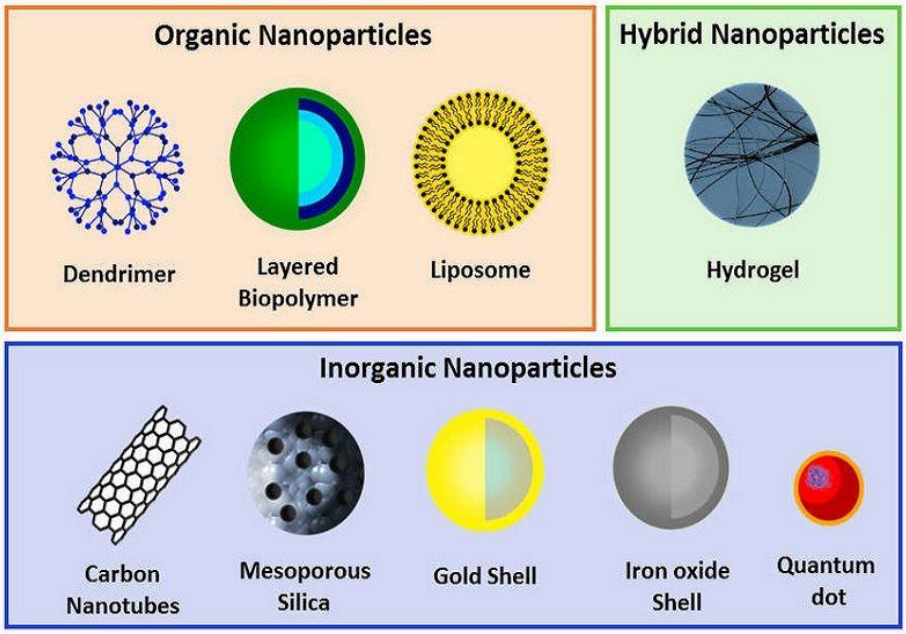

Figure 1.2 - Classification of NPs based on compositions

1.3.1. Quantum Dots

Ekimov and Onushenko were the first to describe quantum dots (QDs), also known as nanoscale semiconductor crystals, in a glass matrix. In brief, QDs are exceptionally little particles in the scope of just a few nanometers. They are little to such an extent that their optical and electronic properties contrast essentially from those of their bigger particles. These nanoscale particles, which are usually made of semiconductor materials, firmly bind either electrons or electron holes. QDs discharge light of explicit frequencies when power or light is concerned with them. In semiconductor materials[3], absorption of light excites an electron from the valence band to the conduction band, thus generating a hole in the valence band. The hole and the electron generate exciton, which is essentially an electron-hole pair. At the point when the excited electron relaxes

back to the ground state, and the exciton's energy is emitted as light or fluorescence, this whole phenomenon is known as exciton recombination. As the confinement energy depends upon the size of various QDs, both absorption as well as the emission of these QDs can be optimized by varying the size of the QDs during their synthesis.[4,5] The larger size dots absorb and emit lower energy and the spectrum shift towards the orange-red region, whereas the smaller size dots absorb and emit higher energy i.e. bluer light. As a result, a heterogeneous mixture of particles with different sizes manifests excitation wavelength-dependent emission, which is commonly known as multicolor emission. These size-tunable optical properties provide the QDs a great advantage over the common organic fluorophores.[3]

Moreover, they are bright and much more photostable than most of the available fluorescence probes. Since then, the area of QDs has been gradually expanding, prompting a surge in interest in the creation of nano-theranostics platforms capable of simultaneous sensing, imaging, and treatment. With important results previously published in the domains of sensors[4], drug administration, and biomedical imaging, QDs offer a lot of potential for such applications.

1.3.2.1. CdTe QDs

CdTe quantum dots (QDs) are an imperative II–VI group semiconductor material with a low bulk bandgap (1.5 eV), a large excitation Bohr radius (7.3 nm), and size dependant characteristics, making them useful in a broad range of applications. CdTe QDs have good crystallinity and emit over the electromagnetic spectrum, from the green to red region (450-700 nm), with a high luminous quantum yield (QY) of 20-90 %. Thiol-containing substances such as 3-mercaptopropionic acid (MPA), glutathione (GSH), mercaptosuccinic acid (MSA),

thioglycolic acid (TGA), and cysteine (CYS) are commonly used as ligands during the fabrication of CdTe QDs in aqueous media. The QY of QDs is typically influenced by the pH of the solution; in acidic media, Cd^{+2} and excess ligand will deposit on the surface of QDs in the reaction medium, forming a shell-layer structure made up of ligand Cd-complexes. These ligand-Cd complexes effectively block the nonradiative exciton pathway and improve the QY of QDs.[6–9]

1.3.2. Carbon Dots

For years, carbon dots (CDs) have piqued researchers' curiosity as a special type of nanomaterial-based on carbon. CDs are a type of quasi-0D material based on carbon with the size of less than 20 nm with fluorescence as an inherent feature. Carbon nanoparticles having fluorescence behaviour were discovered accidentally during the single-walled carbon nanotubes purification in 2004[10].Yang's team used citric acid (CA) and ethylenediamine as precursors in 2013 and used a one-step hydrothermal technique to synthesize polymer-like CDs with QY up to 80%.[11] These CDs have a range of applications in various research fields such as synthetic chemistry, bioimaging, delivery of the drug, and biosensing. These nanomaterials are water-soluble, have minimal toxicity, and have cheap manufacturing costs. They also exhibit tunable fluorescence excitation and emission. CDs are physicochemical and photochemically stable and also have good biocompatibility.

1.3.3. Polyelectrolytes

Polyelectrolytes are simply polymers that are water-soluble due to the presence of ionic charges along their polymer chain. They are commonly used in the research of complex coacervation. They are classified as linear or branched macromolecule chains that have a large number of ionic groups in their structure. They are usually soluble in a polar solvent, generally water. In positively (or negatively) charged polyelectrolyte solution, a single species polymer with random polydispersity and one species of counter-ions which are small ions with the oppositely charged sign to that of macromolecular charge is present. The charge of counter-ion and macromolecular structure must be equivalent to attain the condition of electroneutrality.

The commonly used polyectrolytes are polyethylenimine (PEI), Spoly(acrylic acid) (PAA) poly(diallyldimethylammonium chloride) (PDADMAC), and poly(sodium 4- styrene sulfonate) (SPS).

Few characteristics of PDADMAC are as follows-

- Poly(diallyldimethylammonium chloride) also, known as polyDADMAC or polyDDA
- It is a high charge density cationic polyelectrolyte.
- The DADMAC monomer is obtained by the reaction of allyl chloride with that dimethylamine.

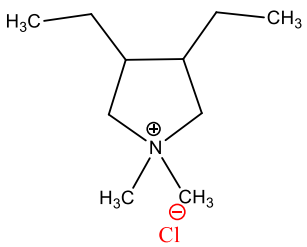

Figure 1.3 Structure of PolyDADMAC

1.4. Coacervate Nanodroplets

Coacervation is an electrostatically induced spontaneous liquid-liquid phase separation (LLPS) process between positively and negatively charged polyelectrolytes.[12,13] Two phases of liquid coexist at the site of coacervation: a thick, polymer-rich phase (droplet phase or coacervate phase) and a highly dilute, polymer-deficient phase defined as the dilute phase. As a result of this procedure, Spherical colloidal coacervate droplets with diameters ranging from a few nanometers to several micrometers are formed. The composition of chemical and polyelectrolytes ratio, equilibration period, ionic strength of the medium and, pH may all be tuned to regulate the size and physicochemical features of coacervates.[14–17] Coacervate has an inherent membrane-free crowded environment. Coacervates have sparked much interest in artificial protocell investigation due to the preferential sequestration of a large range of biomacromolecules like enzymes, dye and, proteins and their intrinsic membrane-less crowding environment.[14–20]

Very recently, we have discovered a methodology for self-assembly of negatively charged nanoparticles like CdTe quantum dots (QDs) or Carbon dots along with positively charged polymer PDADMAC in the aqueous mixture to create a novel class of fundamentally luminous membrane-free porous organic-inorganic hybrid coacervate NDs.[21,22]

Earlier, Mann and co-workers tested the preferential sequestration of the water-insoluble solvatochromic dye, Nile Red, into the PDDA/ATP inorganic coacervate droplet to analyze the relative dielectric constant and found that the interior of these nanodroplets was much more polar as compared to DMSO but less hydrophilic than water.[15] In this regard, In our present work, we investigated the structural and polarity differences between the continuous water phase and

coacervate droplets by adding a DMSO solution of the water-insoluble solvatochromic dye, Nile Red, to a dispersion of QD/CD-embedded coacervate droplets, respectively which is followed by centrifugation process to macroscopically separate the coacervate phases and water phases.

1.5. Solvatochromism

The word solvatochromism is being used to define the pronounced shift in position and occasionally intensity of a UV-visible absorbance band due to the changing the medium polarity. Solvent influence has been studied for a long time, and attempts have been made to correlate the position and intensity of UV absorption bands to the solvent's so-called polarity.[23] Various solvents have been effectively characterized using the solvatochromic comparison approach, which is based on the influence of solvent polarity on the electronic excitation energy of indicator dyes. Electrostatic factors play a role in general solute-solvent interactions, which are classified as the induced dipole-induced dipole, dipole-induced dipole, and dipole-dipole. When a molecule's dipole moment rises as a result of excitation, as it does in π - π * transitions, a more polar or polarizable solvent will help to stabilize the excited state compared to the ground state.[24] Due to it, the gap between the ground and excited-state energy is reduced in this situation, and the absorption spectra are red-shifted, which is referred to as positive solvatochromism or a bathochromic shift. Whereas in negative solvatochromism or a hypsochromic (blue) shift, the excited state is less stabilize than the ground state, generally seen in n - π * transitions. Here, we investigated the solvatochromic effect on the absorption band of water-insoluble dye, Nile Red, in various solvents.

Chapter 2

Experimental Section

2.1. Materials

Cadmium chloride ($CdCl_2$), sodium borohydride ($NaBH_4$), trisodium citrate ($Na_3C_6H_5O_7.2H_2O$), sodium tellurite (Na_2TeO_3), mercaptosuccinic acid (MSA), poly(diallyldimethylammonium chloride) (PDADMAC, MW = 100,000−200,000), hellmanex III, Citric acid monohydrate (99.5%), sodium hydroxide (NaOH), Ethylenediamine (EDA, 99.5%), Nile red (NR), and the Pur-A-Lyzert dialysis kit (molecular weight cutoff 3.5 kDa) were procured from Sigma-Aldrich. A Millipore (Milli-Q integral) water filter system provided Milli-Q water.

2.2. Synthesis of MSA-Capped CdTe QDs

The earlier reported process[25,26] was used to synthesize colloidal MSA-capped CdTe QDs. Briefly, In a one-necked round bottom flask, 4 mL of 0.04 M $CdCl_2$ was first diluted to 50 mL Milli-Q water. Afterward, with constant stirring at room temperature, trisodium citrate dihydrate (100 mg), mercaptosuccinic acid (50 mg), 0.01 M Na_2TeO_3 in 1 mL Milli-Q water, and $NaBH_4$ (50 mg) were added. The stirring was sustained until the mixture color turned green. The flask mixture was then connected to a condenser and refluxed under open-air conditions for 25 min and 5.0 hours to get green-emitting and red-emitting QDs, respectively. To eliminate unreacted starting materials and excess free MSA ligands, the resulting mixture of reaction was filtered using dialysis (molecular weight cutoff of 3.5 kDa) for 24 hours in Milli-Q water. For later use, the purified QD was kept at 4 °C. Earlier published literature[3] was used to determine the stock solution concentration of as-synthesized QD.

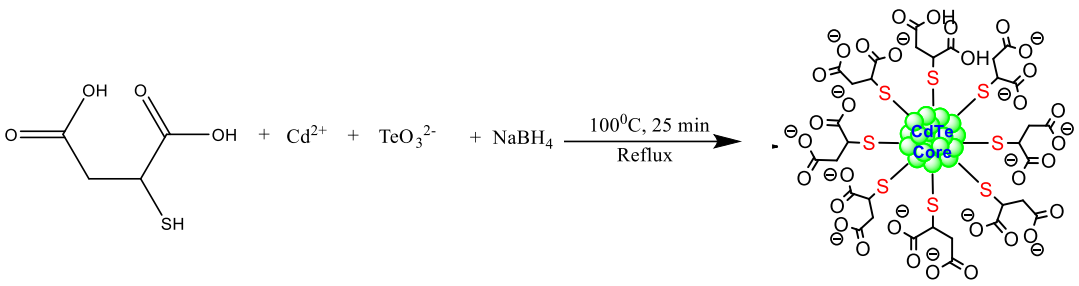

Scheme 2.1 -Schematic representation of synthesis of MSA-capped CdTe QDs

2.3. Synthesis of CDs

We synthesized colloidal CDs using earlier reported methods.[27,28] To summarise, in 10 mL of Milli-Q water, citric acid (1.015 g) was dissolved by sonicating it for 5 minutes. After complete dissolving, ethylenediamine (335 µL) was added to the mixture and again sonicated for 5 minutes. The solution was then transferred to a 25 mL Teflon-padded autoclave and then heated at 200 °C for 5 hours. After 5 h, The reactor was then naturally cooled at normal temperature. To eliminate unreacted starting materials, the resulting mixture of the reaction was filtered using dialysis (molecular weight cutoff of 3.5 kDa) for 24 hours in Milli-Q water. For later use, the purified CDs were kept at 4 °C.

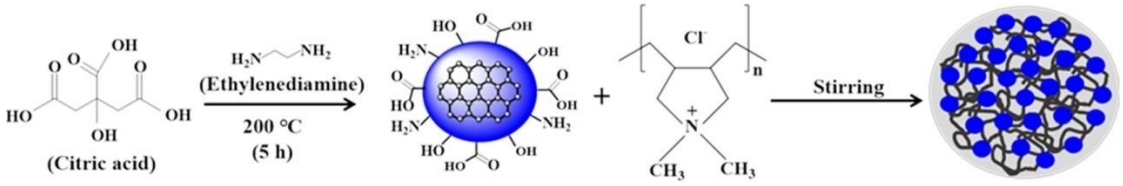

Scheme 2.2 - Schematic representation of synthesis of CDs

2.4. Fabrication of Nanodroplets

2.4.1. QDs-embedded NDs

We have fabricated QD-embedded NDs at two different polymer concentrations i.e. 25.6 μM and 130.0 μM, which corresponds to turbid point 1 (T_1) and turbid point 2 (T_2), while keeping the concentration of QDs constant at 0.33 μM**,** for the present study. The NDs were fabricated at room temperature. Before any experiments, all of the binary mixes were equilibrated for 4 hours at room temperature. Due to equilibration, stable, spherical, well-dispersed nanodroplets were obtained.

2.4.2. CDs embedded NDs

For the present study, we have synthesized CD-embedded NDs at two different polymer concentrations i.e., 32 μM and 64 μM, which corresponds to turbid point 1 (T_1) and turbid point 2 (T_2), keeping the concentration of CD constant (0.06 mg/mL). The NDs were fabricated at pH 10. The polymer-CD binary mixture was equilibrated for 18 h before any measurements. Centrifugation (10000 rpm, 30 min) was used to separate the equilibrated ND dispersions from free CD and PDADMAC.

2.5. Partitioning of dye molecules

We calculated the equilibrium partition coefficient to show how the current hybrid droplets preferentially sequester organic dyes. The bulk coacervate phase of QD-embedded NDs and

CD-embedded NDs was collected from a turbid binary solution of T_1 and T_2. A separate dye stock solution was made in DMSO. The volume required from the Nile Red stock solution in DMSO to reach the final functioning concentration of 3.33 μM (Nile Red) was introduced to the coacervate solution. After the introduction of dye, these binary solutions were equilibrated for 2 h. Afterward, these binary mixtures were centrifuged for 30 min at 10000 rpm to isolate the supernatant phase from the coacervate phase. Centrifugation was used to isolate the free dye concentration, i.e. present in the supernatant, from the solution that was not sequestered inside the droplet. UV-vis spectroscopy was used to measure the concentration of dye in the supernatant. The partition coefficient (*K*) was determined as the ratio of loaded dye concentrations in coacervates to free dye concentrations in the supernatant.

2.6. Instrumentation

A Varian UV-vis spectrophotometer (Carry 100 Bio) was used to measure the electronic absorption spectra in a quartz cuvette (1 cm x 1 cm). A Fluoromax-4 spectrofluorometer (HORIBA Jobin Yvon, model FM-100) was used to take steady-state PL measurements with a 5 nm excitation/emission slit width. For the microscopy experiment solutions, were deposited and dried on a properly cleaned coverslip for confocal imaging measurements. Coverslips were cleaned using chromic acid first (15 min), then washed with Milli-Q water. After that, the rinsed coverslips were treated using 2% Hellmanex III (15 min). Finally, coverslips were washed thoroughly with Milli-Q water, rinsed with methanol, and dried in a vacuum oven. An inverted confocal microscope (Olympus, model no. FV1200MPE, IX-83) having an oil immersion objective (100×, 1.4 NA) was used to perform confocal laser scanning microscopy (CLSM) on a

properly cleaned coverslip. The samples were excited using diode lasers (405, 488, and 559 nm). In the optical path, suitable dichroic and emission filters (blue channel, 410-490 nm; green channel, 490-550 nm; red channel, 570-670 nm) were used to capture images. Solutions were deposited on a properly cleaned and dried overnight in a desiccator.

Chapter 3

Results and Discussions

3.1. Solvents' Effect on Nile Red

For the present study Nile Red was chosen as a model dye due to its insolubility in aqueous phase. Nile Red is a water-insoluble solvatochromic dye that can be sequestered inside the coacervate core. Using UV and FL spectroscopy (Figure 3.1), we characterized Nile Red in various solvents having different polarities. For 0.66 μM concentration of Nile Red in DCM, IPA, Ethanol, DMSO, and H_2O, the UV absorption peak appears at 540 nm, 544 nm, 548 nm, 552 nm, and 591 nm, respectively, while the PL peak appears at 608 nm, 619 nm, 638 nm, 632 nm, and 658 nm, respectively (Table 3.1).

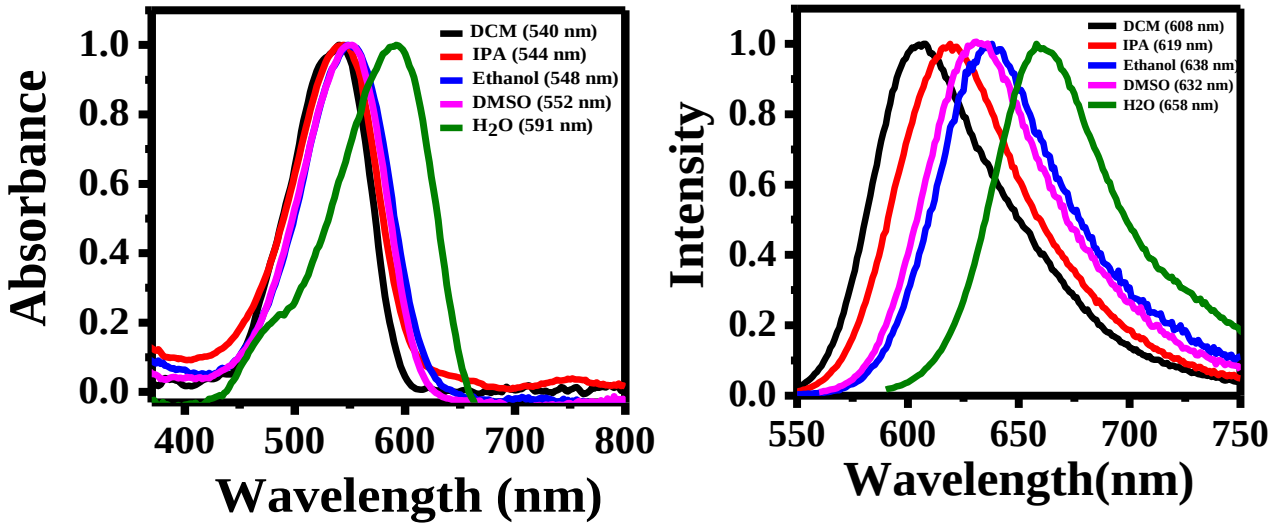

Figure 3.1 Normalized Absorption and Emission spectra for Nile Red. The solvents are DCM, isopropyl alcohol (IPA), ethanol (EtOH), DMSO, and water.

Solvent	Dielectric Constant	Refractive index	U.V Peak	P.L. Peak
DCM	9.1	1.424	540 nm	608 nm
IPA	19.92	1.377	544 nm	619 nm
Ethanol	24.55	1.361	548 nm	638 nm

DMSO	46.7	1.479	552 nm	632 nm
Water	81	1.333	591 nm	658 nm

Table 3.1 - Absorption and emission spectrum peak position of Nile Red. The solvents are DCM, isopropyl alcohol (IPA), ethanol (EtOH), DMSO, and water.

Figure 3.1 shows the changes in the U.V. and P.L. spectra of Nile Red in the presence of different polarities solvents. The solvent dependent study of Nile Red clearly shows prominent changes. The red shift observed in its absorption and emission spectra, when moving from non-polar to polar solvents can be attributed to the much more stabilization of its excited states in the polar medium.

3.2. Characterization of QDs and QD-embedded NDs

The dialysis purified CdTe-QDs were studied using various techniques like UV-vis spectroscopy, PL spectroscopy, FTIR, and confocal laser scanning microscopy. Figure 3.2 A and B show the excitonic emission, and absorption spectrum of MSA Capped CdTe-QDs in Milli-Q water. The exciton band maximum at 490 nm (Figure 3.2 A) corresponds to the broad absorption spectrum of CdTe-QDs, and the sharp emission spectrum (Figure 3.2 B) corresponds to the 517 nm centered PL band obtained upon excitation at 450 nm. FTIR spectroscopy was used to confirm the covalent binding of MSA ligands to the surface of QDs.[21,25] Mixing positively charged PDADMAC with negatively charged MSA-capped QDs in Milli-Q water started the nanodroplets fabrication. These coacervates are inherently luminous due to the presence of QDs. CLSM images of coacervate nanodroplets produced from QDs are shown in Figure 3.2. The

generation of identical spherical nanodroplets can be seen in the differential interference contrast (DIC) pictures of NDs (Figure 3.2 C, D). More significantly, the green fluorescence channels demonstrate a characteristic green luminescence that comes exclusively from the inside of NDs. These results clearly show the existence of self-assembled QDs within these coacervates.

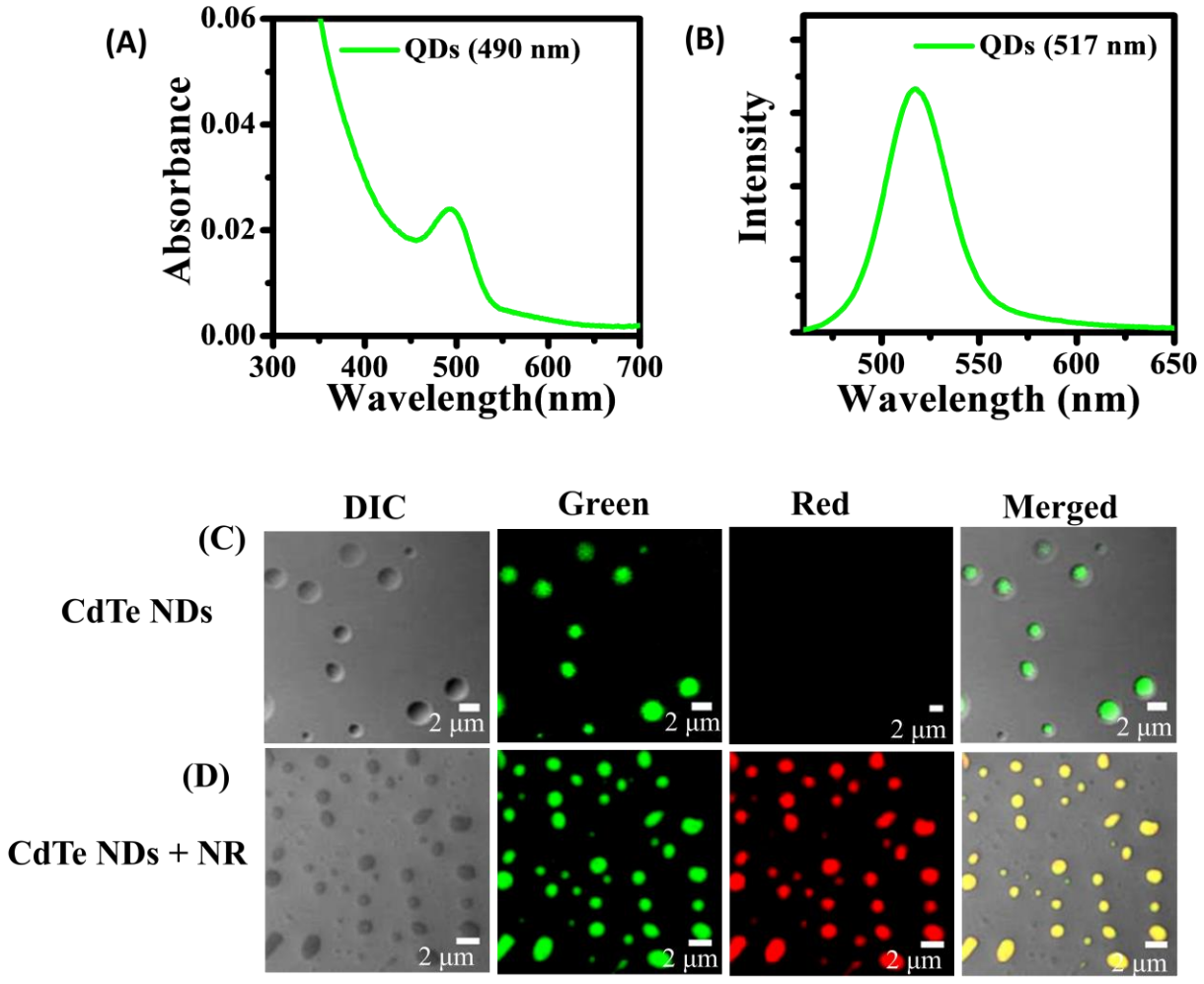

Figure 3.2 - **(A)** Absorption and **(B)** PL spectra (λex = 450 nm) of QDs. Confocal images (DIC, green and red fluorescence, and merge) **(C)** of QD-embedded coacervate NDs **(D)** and sequestrated coacervate nanodroplets in the T_2 regions.

3.3. Characterization of CDs and CD-embedded NDs

The dialysis purified CDs were characterized using various techniques like UV-Vis spectroscopy, PL spectroscopy, and confocal laser scanning microscopy. Figure 3.3 A & B shows the excitonic emission and absorption spectrum of CDs in Milli-Q water. The exciton band maximum at 340 nm and the sharp emission spectrum centered at 441 nm were obtained upon excitation at 340 nm Figure (3.3 A, B). Mixing positively charged PDADMAC with CDs in Milli-Q water at room temperature started the nanodroplet fabrication. These coacervates are inherently luminous due to the presence of CDs. CLSM images of coacervate nanodroplets produced from CDs are shown in Figure 3.3 C & D. The generation of identical spherical nanodroplets can be seen in the differential interference contrast (DIC) pictures of NDs. More significantly, the blue fluorescence channels demonstrate a characteristic blue luminescence that comes exclusively from the inside of NDs. These results clearly show the existence of self-assembled CDs within these coacervates.

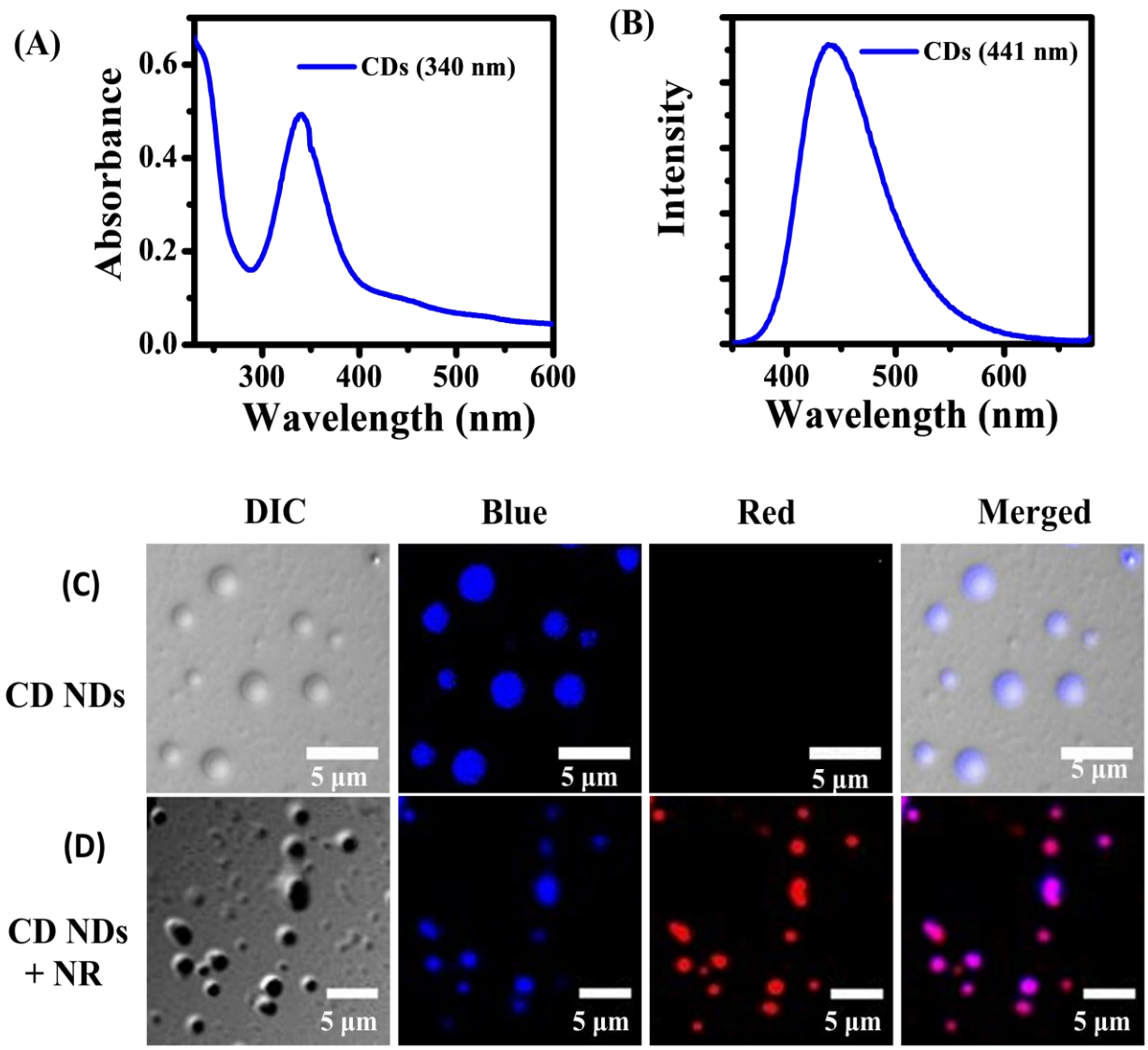

Figure 3.3 - **(A)** Absorption and **(B)** PL spectra (λex = 340 nm) of CDs. Confocal images (DIC, blue and red fluorescence, and merge) **(C)** of CD-embedded coacervate NDs **(D)** and sequestrated coacervate nanodroplets in the T_2 regions

3.4. Sequestration of Nile Red

Coacervates sequester a wide range of organic and inorganic compounds within their porous

membrane-less structure.[14,15,21] Earlier, it has been demonstrated that both electrostatic and hydrophobic interactions of foreign guest molecules and coacervate enhance this preferential sequestration. We exploited the intrinsic polarity differences between the T_1 and T_2 of QD/CD-embedded coacervate NDs and continuous water phase for the preferential sequestration of water-insoluble Nile Red guest molecules. We calculated the equilibrium partition coefficient to show how the current QD/CD-embedded droplets preferentially sequester organic dyes. Equilibrium partition coefficients (K = $[solute]_{in}$/ $[solute]_{out}$) for diverse solutes, including dyes, small and large biomolecules, and inorganic nanoparticles, were determined by UV-Vis spectroscopy. We determined the equilibrium partition coefficients for the preferential sequestration of Nile Red in QD/CD-embadded NDs (Figure 3.4).

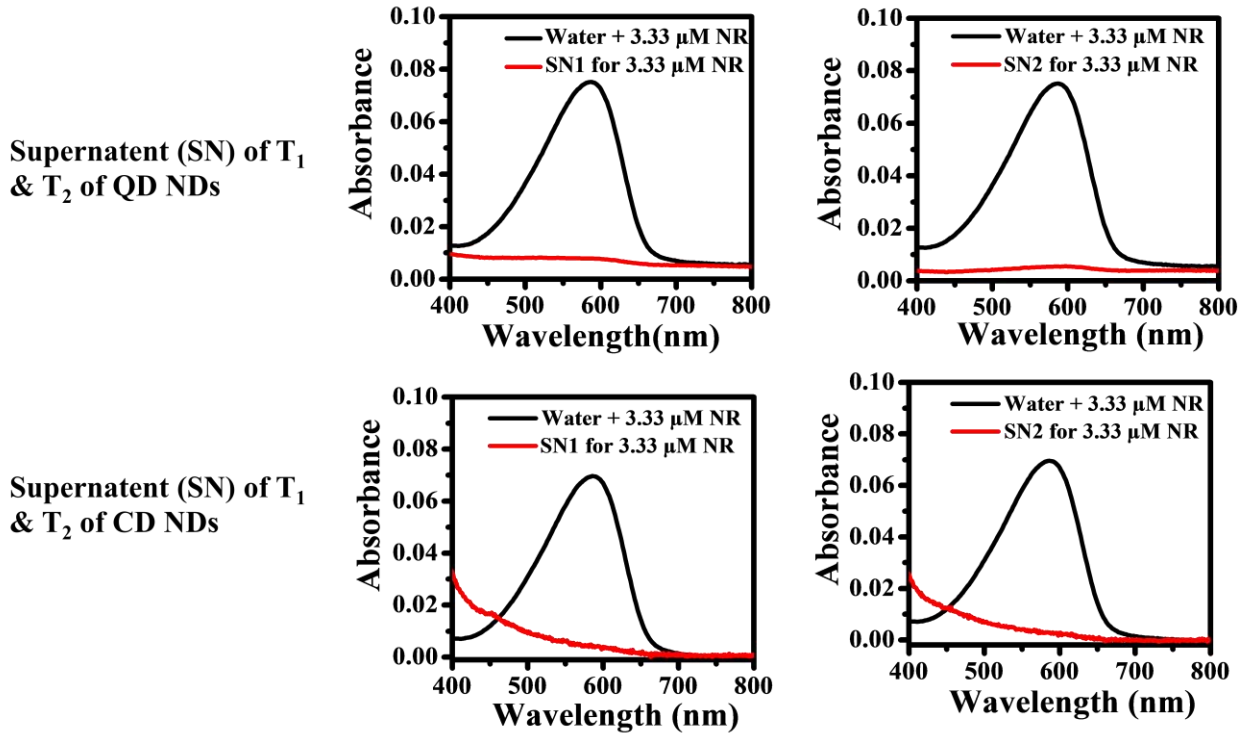

Figure 3.4 - UV-Vis spectra of Nile Red in water (black line) and in aqueous supernatant (red line) of NDs

NDs System	Concentration of Nile Red (μM)	Partition Coefficients (*K*)
T_1 QD-embedded NDs	3.33 μM	8.07 ± 0.45
T_2 QD-embedded NDs	3.33 μM	13.54 ± 0.74
T_1 CD-embedded NDs	3.33 μM	17.18 ± 1.98
T_2 CD-embedded NDs	3.33 μM	28.98 ± 2.44

Table 3.2 - Estimated Equilibrium Partition Coefficients (*K*) of Nile Red in the Presence of T_1 and T_2 NDs system of QD and CD

Table 3.2 shows the equilibrium partition coefficients (*K*) for Nile Red calculated using UV-Vis spectroscopy. These *K* values showed the Nile Red loading inside the QD/CD-embedded NDs. We performed a confocal imaging experiment with T_2 NDs of QD as well as CD. In the absence of dye, both types of NDs did not exhibit red luminescence behaviour in the red channel of confocal imaging (Figures 3.2 & 3.3). But when we sequestrated Nile Red inside the droplet and performed confocal imaging, QD-embedded NDs exhibited red luminescence behaviour (Figure 3.2 D) that comes exclusively from inside the NDs; also same behaviour was observed for CD-embedded ND (Figure 3.3 D). This confirmed the guest Nile Red dye loading inside the coacervate interior. Generally, variable solvation and complementary interactions between the coacervate and aqueous media were used to rationalize the sequestration of tiny organic molecules, proteins, or hybrid nanoparticles. This was in line with the sequestration properties of uncharged, water-insoluble Nile Red (Fig. 3.4) and showed that van der Waals interactions between dye molecules and NDs complex might play a role in the coacervate droplets' uptake

behaviour.

3.5. Nature of Confined Environment of NDs

UV-Vis spectra of Nile Red sequestered into the coacervate phase (Figure 3.4) and confocal images of sequestered dye inside the coacervate nanodroplets of QD/CD-embedded (Figure 3.2 D & 3.3 D) confirmed the sequestration of dye inside the confined environment of NDs. Earlier, S. Mann and coworkers demonstrated the polarity behaviour of PDDA/ATP organic coacervate droplet for Nile Red guest molecule and observed that Nile Red dye gave an absorption peak at 552 nm, and when it sequestered into the coacervate, it gave the absorption peak at 606 nm, this indicated that coacervate interior was much more polar than DMSO but less hydrophilic than pure water.[15] Similarly, we investigated this by adding a DMSO stock solution of the water-insoluble, solvatochromic dye, Nile Red, to QD/CD-embedded coacervate droplets. Corresponding UV-Vis spectra of Nile Red dye give an absorption peak at 552 nm and in DMSO at 591 nm in water (Figure 3.1). the absorbance spectrum of Nile Red shows a red shift from 552 nm (DMSO) to 598 nm in the coacervate phase of QD-embedded NDs. Similar red shift in the absorption of Nile Red was observed in the coacervate phase of CD-embedded NDs. (Figure 3.5). It indicated that the droplet interior is significantly much more polar than DMSO and slightly more polar than water.

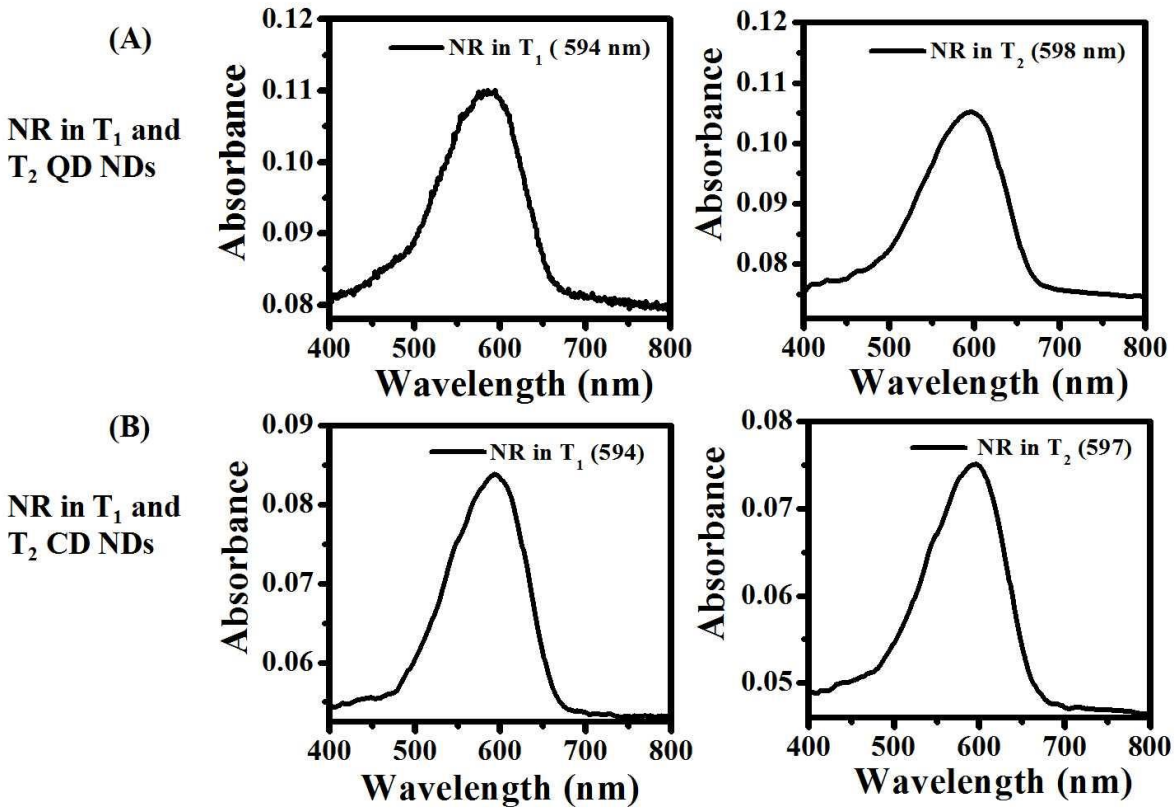

Figure 3.5 - UV-Vis absorption spectra of Nile Red in T_1 & T_2 of **(A)** QD-embedded NDs **(B)** CD-embedded NDs

NDs System	U.V Peak
T_1 QD-embedded NDs	594 nm
T_2 QD-embedded NDs	598 nm
T_1 CD-embedded NDs	594 nm
T_2 CD-embedded NDs	597 nm

Table 3.3 - UV-Vis absorption peak of Nile Red in T_1 & T_2 of **(A)** QD-embedded NDs **(B)** CD-embedded NDs

Chapter 4

Conclusion

In the present work, we have utilized the membraneless architecture of the different hybrid coacervate NDs to study the uptake behaviour of a water insoluble dye i.e., Nile Red inside its microenvironment. The subsequent results were further utilized to study the nature of the microenvironment of these nanoparticle-embedded hybrid NDs. For the present study Nile Red was chosen as a model dye due to its insolubility in aqueous phase. The solvent dependent study of Nile Red clearly shows prominent changes. The red shift observed in its absorption and emission spectra, when moving from non-polar to polar solvents can be attributed to the much more stabilization of its excited states in the polar medium.

Next, two different hybrid coacervate nanodroplets were prepared by the simple mixing of negatively charged QDs/CDs with the positively charged polymer PDADMAC. Our study reveals that these QD and CD-embedded NDs can act as a host to sequester the guest water-insoluble Nile Red inside its confined micro environment. The confocal imaging of Nile Red-loaded NDs clearly shows the presence of Nile Red inside the confined structure of NDs while the absorbance spectrum of Nile Red shows a red shift from 552 nm (DMSO) to 598 nm in the coacervate phase of QD-embedded NDs. Similar red shift in the absorption of Nile Red was observed in the coacervate phase of CD-embedded NDs. These results clearly shows that the microenvironment of these nanoparticle-embedded NDs is more polar as compared to DMSO. Given the variety of characteristics present, our results suggest that these droplets have unique features that allows them to be used in a variety of applications such as bioimaging and drug delivery and also used to resolve the solubility issues of various drugs and dyes in aqueous solutions and various other solutions as well.

References

(1) Biju, V.; Itoh, T.; Ishikawa, M. Delivering Quantum Dots to Cells: Bioconjugated Quantum Dots for Targeted and Nonspecific Extracellular and Intracellular Imaging. *Chem. Soc. Rev.***2010**, *39* (8), 3031–3056. https://doi.org/10.1039/B926512K.

(2) Ekimov, A. I.; Onushchenko, A. A. Quantum Size Effect in Three-Dimensional Microscopic Semiconductor Crystals. *Sov. J. Exp. Theor. Phys. Lett.***1981**, *34*, 345.

(3) *Semiconductor Clusters, Nanocrystals, and Quantum Dots*. https://www.science.org/doi/10.1126/science.271.5251.933 (accessed 2022-05-19).

(4) Chang, J.; Waclawik, E. R. Colloidal Semiconductor Nanocrystals: Controlled Synthesis and Surface Chemistry in Organic Media. *RSC Adv.***2014**, *4* (45), 23505–23527. https://doi.org/10.1039/C4RA02684E.

(5) *Semiconductor Nanocrystals: Structure, Properties, and Band Gap Engineering | Accounts of Chemical Research*. https://pubs.acs.org/doi/10.1021/ar9001069 (accessed 2022-05-19).

(6) Law, W.-C.; Yong, K.-T.; Roy, I.; Ding, H.; Hu, R.; Zhao, W.; Prasad, P. N. Aqueous-Phase Synthesis of Highly Luminescent CdTe/ZnTe Core/Shell Quantum Dots Optimized for Targeted Bioimaging. *Small Weinh. Bergstr. Ger.***2009**, *5* (11), 1302–1310. https://doi.org/10.1002/smll.200801555.

(7) Ma, Y.; Zhang, Y.; Yu, W. W. Near Infrared Emitting Quantum Dots: Synthesis, Luminescence Properties and Applications. *J. Mater. Chem. C***2019**, *7* (44), 13662–13679. https://doi.org/10.1039/C9TC04065J.

(8) Resch, U.; Weller, H.; Henglein, A. Photochemistry and Radiation Chemistry of Colloidal Semiconductors. 33. Chemical Changes and Fluorescence in CdTe and ZnTe. *Langmuir***1989**, *5* (4), 1015–1020. https://doi.org/10.1021/la00088a023.

(9) Resch-Genger, U.; Grabolle, M.; Cavaliere-Jaricot, S.; Nitschke, R.; Nann, T. Quantum Dots versus Organic Dyes as Fluorescent Labels. *Nat. Methods***2008**, *5* (9), 763–775. https://doi.org/10.1038/nmeth.1248.

(10) Xu, X.; Ray, R.; Gu, Y.; Ploehn, H. J.; Gearheart, L.; Raker, K.; Scrivens, W. A. Electrophoretic Analysis and Purification of Fluorescent Single-Walled Carbon Nanotube Fragments. *J. Am. Chem. Soc.* **2004**, *126* (40), 12736–12737. https://doi.org/10.1021/ja040082h.

(11) *Highly photoluminescent carbon dots for multicolor patterning, sensors, and bioimaging - PubMed*. https://pubmed.ncbi.nlm.nih.gov/23450679/ (accessed 2022-05-19).

(12) Buddingh', B. C.; van Hest, J. C. M. Artificial Cells: Synthetic Compartments with Life-like Functionality and Adaptivity. *Acc. Chem. Res.***2017**, *50* (4), 769–777. https://doi.org/10.1021/acs.accounts.6b00512.

(13) Keating, C. D. Aqueous Phase Separation as a Possible Route to Compartmentalization of Biological Molecules. *Acc. Chem. Res.***2012**, *45* (12), 2114–2124. https://doi.org/10.1021/ar200294y.

(14) Frankel, E. A.; Bevilacqua, P. C.; Keating, C. D. Polyamine/Nucleotide Coacervates Provide Strong Compartmentalization of Mg2+, Nucleotides, and RNA. *Langmuir***2016**, *32* (8), 2041–2049. https://doi.org/10.1021/acs.langmuir.5b04462.

(15) Williams, D. S.; Koga, S.; Hak, C. R. C.; Majrekar, A.; Patil, A. J.; Perriman, A. W.; Mann, S. Polymer/Nucleotide Droplets as Bio-Inspired Functional Micro-Compartments. *Soft Matter***2012**, *8* (22), 6004–6014. https://doi.org/10.1039/C2SM25184A.
(16) Pathak, J.; Priyadarshini, E.; Rawat, K.; Bohidar, H. B. Complex Coacervation in Charge Complementary Biopolymers: Electrostatic versus Surface Patch Binding. *Adv. Colloid Interface Sci.***2017**, *250*, 40–53. https://doi.org/10.1016/j.cis.2017.10.006.
(17) Kaushik, P.; Rawat, K.; Aswal, V. K.; Kohlbrecher, J.; Bohidar, H. B. Fluorescent Complex Coacervates of Agar and in Situ Formed Zein Nanoparticles: Role of Electrostatic Forces. *Carbohydr. Polym.***2019**, *224*, 115150. https://doi.org/10.1016/j.carbpol.2019.115150.
(18) Martin, N.; Li, M.; Mann, S. Selective Uptake and Refolding of Globular Proteins in Coacervate Microdroplets. *Langmuir***2016**, *32* (23), 5881–5889. https://doi.org/10.1021/acs.langmuir.6b01271.
(19) Nishida, K.; Tamura, A.; Yui, N. PH-Responsive Coacervate Droplets Formed from Acid-Labile Methylated Polyrotaxanes as an Injectable Protein Carrier. *Biomacromolecules***2018**, *19* (6), 2238–2247. https://doi.org/10.1021/acs.biomac.8b00301.
(20) Lv, K.; Perriman, A. W.; Mann, S. Photocatalytic Multiphase Micro-Droplet Reactors Based on Complex Coacervation. *Chem. Commun.***2015**, *51* (41), 8600–8602. https://doi.org/10.1039/C5CC01914A.
(21) Vaishnav, J. K.; Mukherjee, T. K. Highly Photostable and Two-Photon Active Quantum Dot–Polymer Multicolor Hybrid Coacervate Droplets. *Langmuir***2019**, *35* (36), 11764–11773. https://doi.org/10.1021/acs.langmuir.9b01783.
(22) Singh, S.; Vaishnav, J. K.; Mukherjee, T. K. Quantum Dot-Based Hybrid Coacervate Nanodroplets for Ultrasensitive Detection of Hg2+. *ACS Appl. Nano Mater.***2020**, *3* (4), 3604–3612. https://doi.org/10.1021/acsanm.0c00317.
(23) Reichardt, C.; Welton, T. *Solvents and Solvent Effects in Organic Chemistry*; John Wiley & Sons, 2010.
(24) *Fluorescence Spectrometers | ISS*. https://iss.com/fluorescence/index.html?gclid=Cj0KCQjw1ZeUBhDyARIsAOzAqQL9oDr42CEfcixBbvgoewj2RDQPamZNddGRnR8IbqTWZXFD72mmd_AaAufmEALw_wcB (accessed 2022-05-19).
(25) Vaishnav, J. K.; Mukherjee, T. K. Long-Range Resonance Coupling-Induced Surface Energy Transfer from CdTe Quantum Dot to Plasmonic Nanoparticle. *J. Phys. Chem. C***2018**, *122* (49), 28324–28336. https://doi.org/10.1021/acs.jpcc.8b08757.
(26) Vaishnav, J. K.; Mukherjee, T. K. Surfactant-Induced Self-Assembly of CdTe Quantum Dots into Multicolor Luminescent Hybrid Vesicles. *Langmuir***2019**, *35* (19), 6409–6420. https://doi.org/10.1021/acs.langmuir.9b00357.
(27) Bhattacharya, A.; Chatterjee, S.; Prajapati, R.; Mukherjee, T. K. Size-Dependent Penetration of Carbon Dots inside the Ferritin Nanocages: Evidence for the Quantum Confinement Effect in Carbon Dots. *Phys. Chem. Chem. Phys.***2015**, *17* (19), 12833–12840. https://doi.org/10.1039/C5CP00543D.
(28) Bhattacharya, A.; Chatterjee, S.; Khorwal, V.; Mukherjee, T. K. Luminescence Turn-on/off Sensing of Biological Iron by Carbon Dots in Transferrin. *Phys. Chem. Chem. Phys.***2016**, *18* (7), 5148–5158. https://doi.org/10.1039/C5CP05890B.